

Diffraction from an edge in a self-focusing medium

Wenjie Wan, Dmitry V. Dylov, Christopher Barsi, and Jason W. Fleischer*

Department of Electrical Engineering, Princeton University, Princeton, New Jersey 08544, USA

*Corresponding author: jasonf@princeton.edu

Received March 8, 2010; revised June 15, 2010; accepted June 17, 2010;
posted July 30, 2010 (Doc. ID 124606); published August 13, 2010

We experimentally demonstrate diffraction from a straight edge in a medium with self-focusing nonlinearity. Diffraction into the shadow region is suppressed with increasing nonlinearity, but mode coupling leads to excitations and traveling waves on the high-intensity side. Theoretically, we interpret these modulations as spatially dispersive shock waves with negative pressure. © 2010 Optical Society of America

OCIS codes: 190.4420, 050.1940.

Diffraction from a straight edge is a fundamental phenomenon that practically defines the separation between wave and ray optics. In terms of Fourier optics, diffraction acts as spatial dispersion, altering angular propagation by changing the phase relationship between different components of the signal. In a completely different context, phase mixing can result from nonlinearity, e.g., through self- and cross-phase modulation. It is obvious then that nonlinearity will have an effect on diffraction [1] and diffractive elements [2–4]. Despite this, nonlinear diffraction from boundaries and obstacles has received scant attention. For propagation in self-defocusing media, understanding is aided by considering the optical flow in fluid terms, where intensity disturbances can be described as dispersive shock waves [5–7]. For self-focusing media, the dynamics are complicated by modulation instability (MI), which competes with fringes driven by the edge [8]. Here, we circumvent this problem by using partially spatially incoherent light, which suppresses MI [9,10], but still allows for nonlinear wave coupling [11] and modified diffraction [12]. We show that nonlinearity inhibits diffraction into the shadow region but triggers traveling waves on the high-intensity side. In fluid terms, the dynamics represents an odd type of shock wave with negative pressure [6,13].

The spatial wave dynamics can be modeled by a nonlinear Schrödinger equation:

$$i \frac{\partial \psi}{\partial z} + \frac{1}{2k_0} \nabla_{\perp}^2 \psi + \frac{k_0 \Delta n(|\psi|^2)}{n_0} \psi = 0, \quad (1)$$

where $\psi(x, y, z)$ is the slowly varying amplitude of the electric field as it propagates along the z axis, $k_0 = 2\pi n_0/\lambda$ is the wavenumber for light with wavelength λ/n_0 in a homogeneous medium of refractive index n_0 , and Δn is a nonlinear index change that depends on the intensity $|\psi|^2$. For example, the cubic Schrödinger equation results from using the Kerr nonlinearity $\Delta n = n_2 |\psi|^2$, where n_2 is the nonlinear coefficient.

We are interested in the nonlinear diffraction from a sharp, steplike edge:

$$\psi(x, 0) = \begin{cases} a & x < 0 \\ 0 & x > 0 \end{cases},$$

where a is the initial field on the bright side of the edge. It is helpful to express Eq. (1) in (nonlinear) eikonal

form by applying the polar transformation $\psi(x, z) = \sqrt{\rho(x, z)} \exp[iS(x, z)]$. Separating real and imaginary components and writing $v = \nabla S$ gives

$$\frac{\partial \rho}{\partial z} + \nabla_{\perp}(\rho v) = 0, \quad (2)$$

$$\frac{\partial v}{\partial z} + v \nabla_{\perp} v = \frac{1}{\rho} \nabla_{\perp} P + \frac{1}{2} \nabla_{\perp} \left(\frac{1}{\sqrt{\rho}} \nabla_{\perp}^2 \sqrt{\rho} \right). \quad (3)$$

These equations are reminiscent of those for ideal fluid flow, where the intensity ρ is the “density” of the optical fluid, the phase gradient v is an effective velocity, and the (Kerr) nonlinearity corresponds to a fluid pressure $P = n_2 \rho^2 / 2n_0$. They express the intuitive notions that positive (negative) nonlinearity causes light to flow toward (away from) the induced refractive index defect, while diffraction always gives an outward force. For highly dynamic situations, however, the competing spatial gradients can lead to counterintuitive flow: self-defocusing can lead to compression and focusing [14], while self-focusing can lead to outwardly radiating waves [6,15]. The formal interpretation in terms of dispersive shock waves (DSWs) follows from the convective derivative in Eq. (3).

Ideally, negative-pressure DSWs occur for purely coherent waves, as shown in simulations of Eq. (1) [Fig. 1 (obtained using a split-step Fourier beam propagation code)]. In the linear case, Fig. 1(a), the intensity pattern is simple diffraction from a straight edge, with broadening on the lower side and small ripples on the higher side. In the nonlinear case, Fig. 1(b), propagation results in a distinctive soliton train characteristic of DSWs [8,16]. The evolution is sequential: the edge is attracted to the high-intensity region in the center (drawn by the negative pressure) and “shocks” the background into the radiation of more waves.

Practically, self-focusing nonlinearity gives rise to modulation instability, in which a broad beam becomes unstable to intensity perturbations [Fig. 1(c)]. This effect occurs simultaneously with nonlinear diffraction from the edge and, indeed, can be triggered by it. A comparison of the effects is shown in Fig. 1. Without noise, the edge wave is a dispersive shock, similar to the self-defocusing case [5], with a compact, smoothly varying envelope in both real space and Fourier space [Fig. 1(b)]. With noise, the output profile depends on the propagation

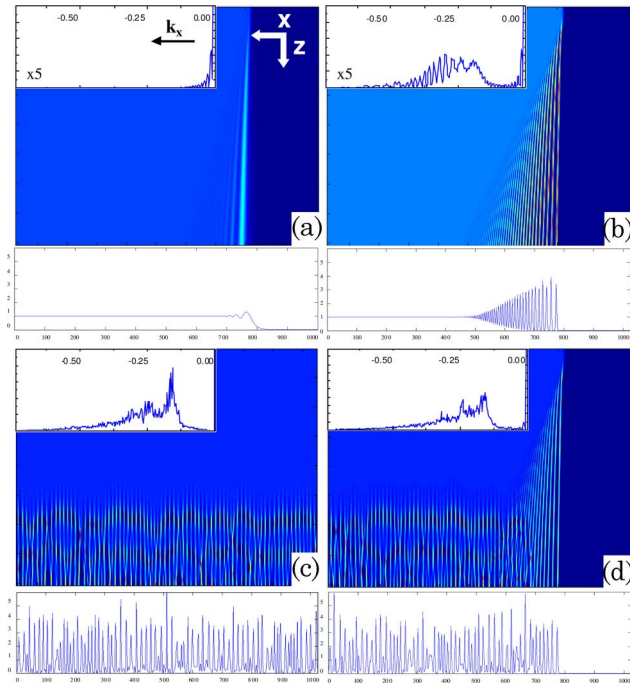


Fig. 1. (Color online) Simulation of Fresnel diffraction from a sharp edge. Shown are top-view evolutions and output cross sections of (a) linear diffraction, (b) nonlinear diffraction without noise, (c) modulation instability without an edge, and (d) nonlinear edge diffraction with noise. Insets show power spectra of output.

distance [Fig. 1(d)]. Initially, the edge wave is dominant and there is a clear separation of behavior. In particular, the linear, nonlinear, and unstable dynamics occupy their own spectral windows. This directly implies that the edge excites its own traveling (shock) waves and is not a simple mode growth process, e.g., modulation instability seeded by the (high frequency) spatial modes of the sharp edge.

To ensure freedom from MI, it has been suggested theoretically to use nonlocality [6,17]. Here, we make the beam partially spatially incoherent and use statistical

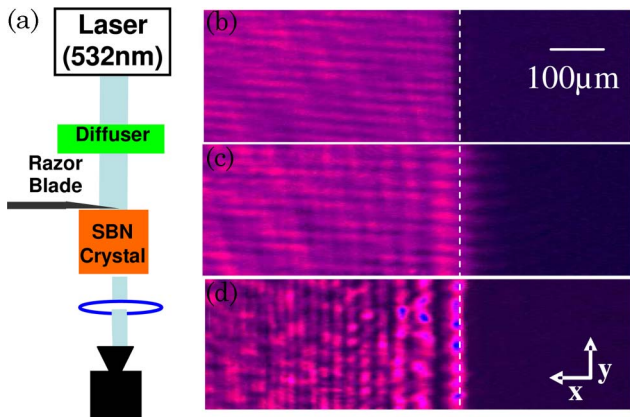


Fig. 2. (Color online) Experiment of nonlinear Fresnel diffraction from a sharp edge. (a) Laser light at 532 nm is made partially spatially incoherent by passing it through a rotating diffuser and is then imaged onto an SBN:75 photorefractive crystal. At the input face, half the light is blocked by a razor blade. Light exiting the crystal is imaged into a CCD camera. (b) Initial stepped intensity at the input face. (c) Linear diffraction at output. (d) Nonlinear diffraction.

dephasing to suppress the onset of instability [9,10]. Experimentally, we use the setup shown in Fig. 2. We first create a partially coherent beam by passing 532 nm laser light through a ground-glass diffuser and then imaging it into a $10 \text{ mm} \times 5 \text{ mm} \times 2 \text{ mm}$ $\text{Sr}_{0.75}\text{Ba}_{0.25}\text{Nb}_2\text{O}_6$ (SBN:75) photorefractive crystal. Rotating the diffuser faster than the response time of the crystal ($\sim 200 \text{ Hz}$ versus 1 Hz) allows a homogeneous intensity input, while adjusting the imaging lens controls the degree of coherence. The initial step condition is created by blocking half the beam with a razor blade and imaging the edge, while the self-focusing nonlinearity is created by applying a positive voltage bias across the crystal [18]. The photorefractive nonlinearity is saturable, but we operate well below the regime where saturation becomes important. Hence, our system is adequately modeled by a Kerr approximation. Finally, at the exit face of the crystal, the output beam profile is imaged onto a CCD camera.

Figure 2 shows the basic experimental results. In the linear case [Fig. 2(b)], light from the bright side of the edge diffracts into the dark side, creating a gently rippled intensity pattern that smoothly extends into the shadow region. Turning on the self-focusing nonlinearity has three major consequences: (1) suppressed linear diffraction in the dark region, (2) increased propagation into the bright region, and (3) compression and enhancement of the intensity modulations.

Similar mode coupling has been observed recently in the bump-on-tail instability [11] but, in that case, the momentum exchange is symmetric within the distribution. For the shock case here, there is an impulsive kick imparted by the initial profile, resulting in a wave that propagates in the transverse direction. To our knowledge,

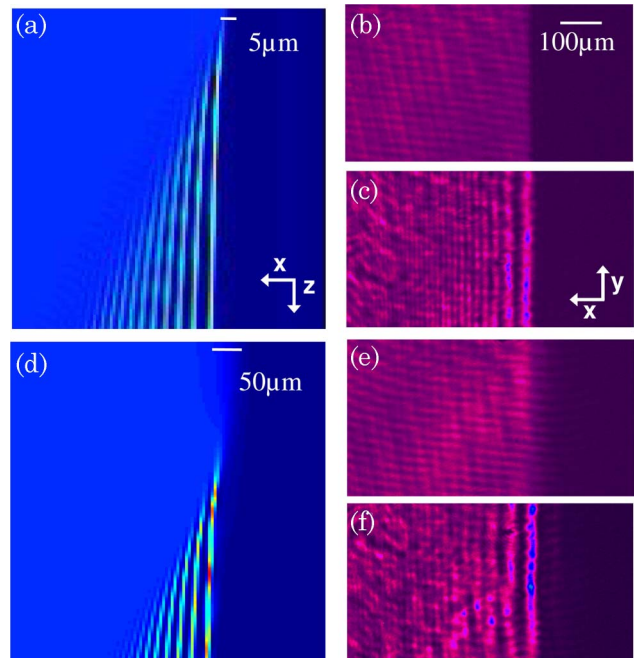


Fig. 3. (Color online) Influence of edge width on nonlinear diffraction. Left column, simulation; right column, experiment. (a)–(c) Results for a sharp edge of $5 \mu\text{m}$ width. (d)–(f) Results for a soft edge of $50 \mu\text{m}$ width. (a), (d) Top views of numerical propagation; (b), (e) experimental input; (c), (f) experimental output for nonlinear diffraction.

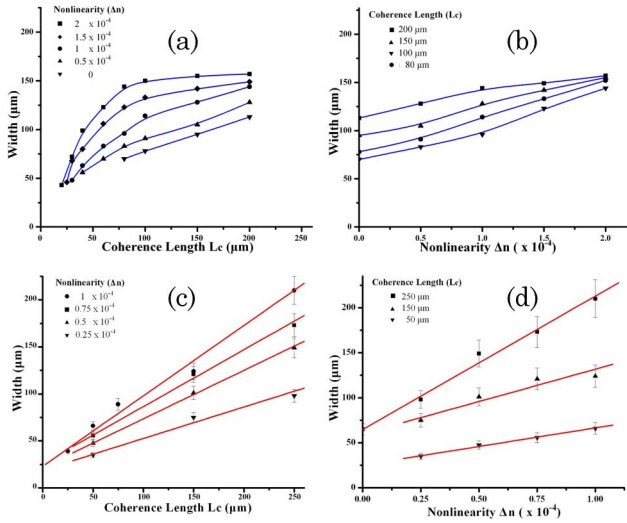


Fig. 4. (Color online) Nonlinear diffraction as a function of nonlinearity and coherence length. (a), (b) Simulation results for shock width as a function of (a) coherence length and (b) nonlinearity. Solid curves are guides to guide the eye. (c), (d) Experimental output pictures for shock width as a function of (c) coherence length and (d) nonlinearity. Solid lines are linear fits to the data.

this is the first demonstration of such a traveling wave in nonlinear statistical optics.

The initial impulse makes nonlinear Fresnel diffraction very sensitive to details of the boundary (Fig. 3), giving it potential for enhanced imaging of edges [19,20]. For a steeper edge, the onset of fringes (wave breaking) is earlier, resulting in a deeper penetration into the high-intensity side, and the lobes are narrower. Interestingly, the propagation speed of the fringes into the high-intensity side, given by the slope dx/dy of the envelope [Figs. 3(a) and 3(d)] remains the same.

The speed of fringe propagation is determined by the pressure (intensity) jump across the interface and the degree of incoherence. A measure is given by the transverse width of the shock wave at the output face. For linear diffraction, the spatial extent of the fringes scales with their visibility, which is directly proportional to the mutual coherence function. For nonlinear diffraction, the influence of coherence can be highly nonlinear [Fig. 4(a)]; however, the strong nonlinearity required to observe this was not possible in the experiment [Fig. 4(b)]. For fixed coherence, the shock width scales linearly for both weak and strong nonlinearity [Figs. 4(c) and 4(d)]. This observation is at odds with the square-root dependence observed for homogeneous diffraction [5] [a velocity

scaling that follows by neglecting the third-order diffraction term in Eq. (3)]. Here, the sharp, nearly discontinuous profile of the edge means that all of the diffraction terms contribute significantly to the dynamics.

In summary, we have considered nonlinear diffraction from a straight edge in a self-focusing medium. We have observed suppressed diffraction inside the shadow region but enhanced fringing and propagation into the bright region. The sharp edge dominated the dynamics, leading to a spatially dispersive shock wave with negative pressure. The results demonstrate the importance of boundary conditions and traveling waves in nonlinear statistical optics and hold potential for enhanced imaging techniques using spatial nonlinearity.

References

1. I. Freund, Phys. Rev. Lett. **21**, 1404 (1968).
2. R. Reinisch and M. Neviere, Phys. Rev. B **28**, 1870 (1983).
3. P. Vincent, N. Paraire, M. Neviere, A. Koster, and R. Reinisch, J. Opt. Soc. Am. B **2**, 1106 (1985).
4. O. Manela and M. Segev, Opt. Express **15**, 10863 (2007).
5. W. Wan, S. Jia, and J. W. Fleischer, Nat. Phys. **3**, 46 (2007).
6. N. Ghofraniha, C. Conti, G. Ruocco, and S. Trillo, Phys. Rev. Lett. **99**, 043903 (2007).
7. E. G. Khamis, A. Gammal, G. A. El, Y. G. Gladush, and A. M. Kamchatnov, Phys. Rev. A **78**, 013829 (2008).
8. S. Chavez-Cerda, M. D. Iturbe-Castillo, and J. M. Hickmann, in *Self-Focusing: Past and Present*, Vol. 114 of Topics in Applied Physics (2009), pp. 517–545.
9. M. Soljacic, M. Segev, T. Coskun, D. N. Christodoulides, and A. Vishwanath, Phys. Rev. Lett. **84**, 467 (2000).
10. D. Kip, M. Soljacic, M. Segev, E. Eugenieva, and D. N. Christodoulides, Science **290**, 495 (2000).
11. D. Dylov and J. W. Fleischer, Phys. Rev. Lett. **100**, 103903 (2008).
12. C. Sun, D. V. Dylov, and J. W. Fleischer, Opt. Lett. **34**, 3003 (2009).
13. V. A. Vysloukh, V. Kutuzov, V. M. Petnikova, and V. V. Shuvalov, J. Exp. Theor. Phys. **84**, 388 (1997).
14. S. Jia, W. Wan, and J. W. Fleischer, Opt. Lett. **32**, 1668 (2007).
15. C. Sun, C. Barsi, and J. W. Fleischer, Opt. Express **16**, 20676 (2008).
16. A. M. Kamchatnov, A. Gammal, F. K. Abdullaev, and R. A. Kraenkel, Phys. Lett. A **319**, 406 (2003).
17. G. Assanto, T. R. Marchant, and N. F. Smyth, Phys. Rev. A **78**, 063808 (2008).
18. D. N. Christodoulides, T. H. Coskun, M. Mitchell, and M. Segev, Phys. Rev. Lett. **78**, 646 (1997).
19. C. Barsi, W. Wan, and J. W. Fleischer, Nat. Photonics **3**, 211 (2009).
20. D. V. Dylov and J. W. Fleischer, Nat. Photonics **4**, 323 (2010).